

## Validation of Fully Automatic Adipose Tissue Segmentation and Volume Quantification

Bryan T Addeman<sup>1</sup>, Melanie Beaton<sup>2</sup>, Robert A Hegele<sup>3</sup>, Abraam S Soliman<sup>3,4</sup>, Curtis N Wiens<sup>5</sup>, and Charles A McKenzie<sup>1,5</sup>

<sup>1</sup>Department of Medical Biophysics, University of Western Ontario, London, ON, Canada, <sup>2</sup>Department of Medicine, University of Western Ontario, London, ON, Canada, <sup>3</sup>The Robarts Research Institute, London, ON, Canada, <sup>4</sup>Biomedical Engineering, University of Western Ontario, London, ON, Canada, <sup>5</sup>Department of Physics, University of Western Ontario, London, ON, Canada

**Introduction:** MRI fat quantification has been shown to be an effective method for measuring body fat content. However, due to signal intensity variations and anatomical complexity, most analysis requires at least some manual input and is often performed on only a subset of collected data. Water and Fat separation techniques such as IDEAL [1] and Lava-Flex [2], (multi-point Dixon imaging) provide images of fat and water that are perfectly registered. As a result, fat signal can be normalized using a Fat-to-Water ratio allowing adipose tissue to be identified *in vivo* by its high fat fraction values [3]. Automated fat volume quantification from a quantitative fat fraction map has the ability to yield accurate, reproducible results over complete imaging volumes. We propose a novel method for the automated quantification and separation of Total Adipose Tissue (TAT), Subcutaneous Adipose Tissue (SAT), and Intra-Abdominal Adipose Tissue (IAAT).

**Methods:** Following REB approval and obtaining informed consent, *in vivo* data were obtained from 24 subjects, including 16 with non-alcoholic fatty liver disease, and 8 healthy volunteers. Transverse abdominal images were collected using an investigational version of IDEAL with varying parameters (General parameters: # echoes = 6, Echo Train Length = 3, 4-10 mm slice thickness, FOV = 48x38 cm, Scan Time = 20 s, matrix = 192x192x28) and coils (Single-channel, 8-channel, and 32-channel) on a GE 3.0 T MR750 (GE Healthcare, Waukesha, WI). In addition, transverse slices of the gluteus maximus and mid-thigh were available for 5 of the patients. Single slices at the L4, mid-gluteus, and mid-thigh levels were segmented with both a manual and automated technique. Manual segmentation was performed using a previously validated connected threshold approach on T2\*-corrected fat images in imageJ [4]. Automated segmentation was completed as follows (see also Figure 1). (1&2) A k-means algorithm was used on T2\*-corrected fat images to separate total tissue volume from background noise. The algorithm splits intensities on the fat-only images into 3 classes, and the lowest intensity class was discarded as noise (air, bone, and water filled regions). (3) The higher intensity classes are converted into binary, and flood filled to create a tissue volume

mask. (4) Using the fat fraction map, pixels inside the volume mask with fat fraction values higher than 60% are located using a connected-threshold algorithm created to define the total adipose tissue (TAT) but exclude unwanted lipids (e.g. bone marrow). (5) Conversely, tissues with high water fractions inside the volume mask are found by locating fat fractions below 50%. The resulting water mask represents only water tissue proximal to the SAT and serves as a general boundary of the peritoneum. (6) The water mask is converted into polar coordinates such that the distal edge of the tissue appears along the bottom of the image. (7) A 3D surface is then fitted to the distal-most edge of the polar water mask, with caution to constrain the smoothness so that areas without water tissue directly adjacent to the subcutaneous fat are bridged. This surface is then converted back into Cartesian coordinates and enclosed resulting in a mask of the intra-abdominal cavity. This mask is then used to split the (4) TAT, into (8) SAT and (9) IAAT. The volume of SAT and IAAT was calculated in litres and as a percentage of the tissue volume mask.

**Results:** Automated segmentation agrees well with manual segmentation (Figure 2). Bland Altman plot (Figure 3) shows no bias between segmentation methods for SAT or IAAT. Results for the gluteus and thighs are similar.

**Discussion:** Automated segmentation can be completed in less than 2 s per slice for a 256x256 image, versus manual segmentation which can take 3-8 min per slice for a trained observer. Fat fractions are unaffected by signal variations due to coil sensitivities and provide a reproducible measure of adipose tissue in single and multi channel acquisitions. Fat fractions also allow for other lipid containing tissue such as bone marrow, and hepatic fat to be omitted due to their lower fat fraction values. Further work needs to be completed to additionally segment retro-peritoneal fat from IAAT.

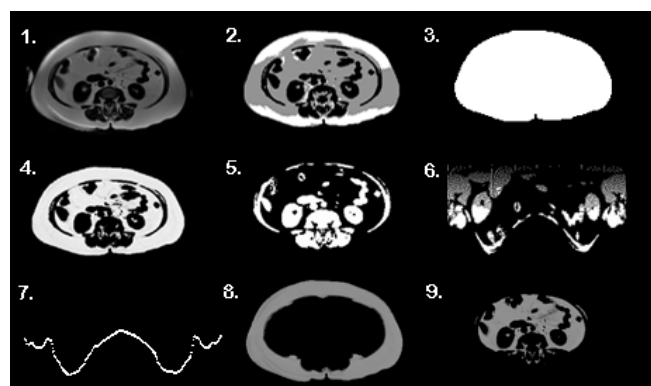


**Figure 1** - Automated Process: (1) Fat-only image (2) K-means segmentation, (3) Volume Mask, (4) TAT, (5) Water Mask, (6) Polar Water Mask, (7) Polar Distal Water Edge, (8) SAT, (9) IAAT

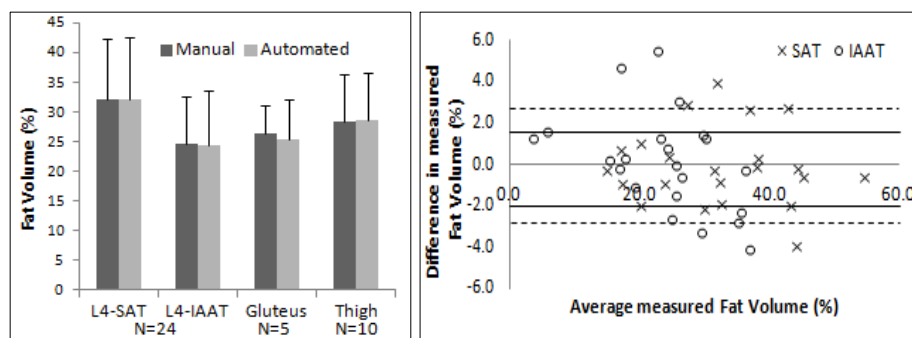


**Figure 2** - Mean fat volume values for manual vs. automated segmentation show excellent agreement. Error bars show standard deviation in measurements.

**Figure 3** - Bland Altman plot comparing manual vs. automated segmentation for SAT, and IAAT. 95% confidence interval lines are shown for SAT (solid) and IAAT (dashed). The plot shows no bias in the automated measurement of either SAT or IAAT.

**Conclusions:** We have demonstrated the ability to automatically segment regional adipose tissue using fat fraction maps, accurately quantifying TAT, SAT, and IAAT. The results are very similar to those obtained by standard manual segmentation methods, but require no manual intervention, are reproducible and can be calculated very rapidly over complete imaging volumes.

**Acknowledgments:** We gratefully acknowledge support from GE Healthcare, NSERC, and the Canada Research Chairs program.

**References:** [1] MRM 2004;51:35-45. [2] MRI 2005;23:977-982 [3] JMRI 2010; 31:1195-1202. [4] JMRI 2011;34(2):474-479.